### **Jefore Ethiopian Journal of Applied Sciences**



ISSN: 3006-6263 (Online); 3080-0617 (Print) Volume 1(1), 2025 Journal homepage: www.jejas.org



Research Paper

### Effect of Tunable Dielectric Properties of the Core on Optical Bistability within Spherical Composite of Metal and Dielectric Nanoparticles

Hawi Aboma <sup>1\*</sup>, Shewa Getachew<sup>2</sup>, Sisay Shewamare<sup>2</sup>

<sup>1</sup>Department of Electrical and Computer Engineering, Wolkite University, Wolkite, Ethiopia

#### **Abstract**

### Article History:

Received: 29 October 2024 Accepted: 27 December 2024 Published online: 06 February 2025

### Keywords:

nanoparticles, optical bistability, active dielectric, dielectric function, enhancement factor

This paper explores how tunable dielectric properties in the core influence the enhancement factor of the local field, induced optical bistability, and its domain in spherical metal-dielectric nanocomposites. Mathematical expressions were derived for the electric potentials governing these nanocomposites using the quasi-static solution of Laplace's equations. The equation for optically induced bistability was obtained through the enhancement factor of the local field equation, incorporating the Drude-Lorentz model. By varying the dielectric properties of the core and the volume of the metal coating on the inclusions, the enhancement of the local field significantly increases at two resonant frequencies when an additional dielectric function is introduced into the active dielectric core. Specifically, the enhancement factor of the local field increases with more dielectric function in the imaginary component of the active dielectric of the core. Furthermore, by comparing three different local field values to a single applied field value, we observe that the bistability region expands with increasing dielectric function in the imaginary part of the active dielectric core, enhancing oscillatory behavior in the system. These findings have potential implications for advancements in optical controls, memory chips, sensor technologies, and logic operations.

#### 1. Introduction

Indeed, experts all around the world are becoming increasingly interested in studying nanoparticles. Numerous investigations have been carried out in this field due to its unique optical properties, which are very different from those of larger bulk materials (Stalmashonak, 2013). Metal-coated core-shell nanocomposites (NCs) are an especially fascinating kind of nanoparticle, where the optical properties of the

nanoparticles are largely determined by the behavior of their surface electrons. The optical function of metal-coated core-shell nanoparticles is significantly influenced by the oscillations of surface electrons within the electric potential created by the positively charged ionic core (Amendola et al, 2017). There are two main reasons why metals and dielectrics are used to regulate light in these structures. Firstly, reducing reflections through interference

\* Corresponding author email: hawi.aboma@wku.edu.et

DOI: <a href="https://doi.org/10.70984/dgr2qq38">https://doi.org/10.70984/dgr2qq38</a>

97

<sup>&</sup>lt;sup>2</sup>Department of Physics, Wolkite University, Wolkite, Ethiopia

cancellation, makes it easier for light to penetrate metals more deeply. Second, it makes light localization possible, which in turn improves the non-linear response (Volz et al, 2012; Zhang & Wang, 2017).

There has been a lot of analysis made during the three decades before today using a variety of methodologies to examine the optical properties of nanoparticles. As one especially promising class of nanoparticle with broad applicability across a variety of scientific and industrial domains, core-shell NCs have surfaced (Bennink et al, 1999). Several variables, including size, metal material, the layout of the core-shell arrangement, and the medium that surrounds it, affect the optical properties of core-shell NCs, which have a metallic shell encircling a dielectric core (Arnold et al., 1990; Mahmudin et al , 2015; Getachew, 2024).

Additional research has shown that, whereas medium and size are critical factors, the shape of core-shell nanoparticles has a major effect on their surface plasmon resonant frequencies (Lisiecki et al, 1996; Getachew & Berga, 2024). The collections of electron disturbances at a nanoparticle's surface, known as plasmon surface resonant frequencies, are highly responsive to particle sizes. The nanoparticles' optical properties can be modified by modulating the vibrations of surface plasmons through the modification of the form of metal-dielectric NCs. Spheroidal NCs have garnered a lot of fascination because of their geometric structure which provides flexibility in optical properties (Lv et al, 2013). However, it is intriguing to notice that most research done so far has mostly concentrated on spheroidal and cylindrical metaldielectric NCs (Getachew et al, 2023; Bergaga et al, 2022; Daneshfar & Bazyari, 2014).

Scientists have also investigated the plasmonic properties of spherical core-shell nanoparticles, including scattering cross-sections, absorption, extinction, and the field improvement factor. They have considered variables such as wavelength, angle, and separation from the center (Piralaee et al, 2018). Numerous studies have already been conducted (Zhu & Zhao, 2016; Chen et al, 2016; Shewamare & Mal'nev 2012) to know the effects of shape, size, material structure, and spatial distributions of NCs on local field enhancement (LFE) factor and induced optical bistability (IOB). However, spherical or cylindrical core-shell NCs have received most of the attention, whereas spheroidal core-shell geometries have received less attention. The effects of the active and passive dielectric characteristics of the host matrices were frequently overlooked, even in ellipsoidal core-shell circumstances when nanocomposites were studied. According to earlier studies, the LFE factor and optical bistability property of metal-dielectric NCs have been investigated using dielectric components coated with metallic substances as the core (Getachew, 2024; Kalyaniwalla et al, 1990; Mahmudin et al, 2015; Gao, 2003).

In many different applications, including nonlinear optical effects, optical sensors, and quantum opt mechanics, the electric field in the local increase in core-shell nanoparticles plays a significant role (Anker et al., 2008; Van Thourhout & Roels, 2010). Among the many varieties of nano-sized particles, induced optical bistability (IOB) is a device of nonlinear optics. The use of IOB in optical machines, quantum technology, optical detection devices, photonic transistors, electronic components, elements, and other applications makes it very attractive (Daneshfar & Naseri, 2017). This study undertakes a comprehensive theoretical and numerical investigation into the effect of adjustable dielectric properties of the core on optical bistability within spherical composites composed of metal and dielectric nanoparticles. Employing the electrostatic approximation for metal-dielectric core in spherical the

nanoparticles, we have explored the effects of introducing an additional imaginary component to the active dielectric core. This modification significantly enhances both the enhancement factor (EF) of the local field and the optical density the metal-dielectric of spherical nanocomposite structure. Consequently, amplifies interactions between nanoparticles and the light, resulting in a broader threshold for optically induced bistability and heightened local field enhancement within the composite.

#### 2. Model and Theory

Take into consideration the nanocomposite system illustrated in Figure 1, which consists of a metal particle with a dielectric function, a spherical-shaped dielectric core with its own dielectric function, and a host matrix containing a dielectric function. The derivation utilizes Laplace's expression in a spherical coordinate system. Here, we intend to utilize these spherical coordinates as a basis to determine the enhancement factor (EF), denoted as A, for a spherical particle. To expedite our deduction, we take into account the two crucial possibilities as follow:

- A. The potential is continuous at the boundary and the same for  $r = r_1$  and  $r = r_2$ .
- B. For  $r = r_1$  and  $r = r_2$ , the displacement vector is continuous and the same at the boundary.

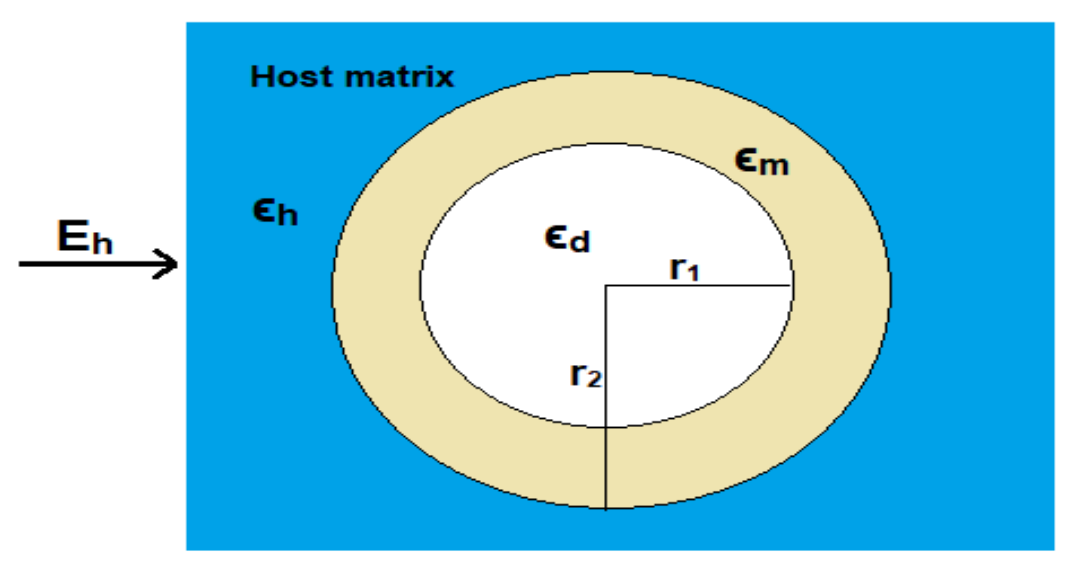


Figure 1: The construction of spherical dielectric particles coated by a metal shell with dielectric function nanoparticles that are implanted in a host matrix with dielectric function  $\varepsilon_h$ 

The allocation of the electric potential inside the system is described by the following formulations, each representing solutions to the Laplace equations for the dielectric core, metal shell, and host matrix, respectively.

$$\Phi_d = -E_h A r \cos \theta, \qquad r \le r_1 \tag{1}$$

$$\Phi_m = -E_h \left( Br - \frac{C}{r^2} \right) \cos \theta, \qquad r_1 \le r \le r_2$$
 (2)

$$\Phi_h = -E_h \left( r - \frac{D}{r^2} \right) \cos \theta, \qquad r > r_2$$
 (3)

Here  $\Phi_d$ ,  $\Phi_m$ , and  $\Phi_h$  are potentials in the dielectric core, metal shell, and the host matrix respectively,  $E_h$  is the applied field,  $\mathbf{r}$  and  $\theta$  are the spherical coordinates of the observation point (the z-axis is chosen along the vector  $E_h$ ),  $r_2$ ,  $r_1$  are radii of the dielectric core and the metal shell, respectively.

The solutions are found using Laplace's equations for the metal-dielectric inclusion and

the host matrix, respectively. The factor of local field enhancement (LFE) of the tiny spherical metal, or the mysterious coefficient A, was finally determined. The scalar potential can be used to derive the electric field both inside and outside the sphere  $\Phi_d$  and  $\Phi_m$ .

$$E_d = \nabla^2 \Phi_d = 0 \tag{4}$$

$$E_m = \nabla^2 \Phi_m = 0 \tag{5}$$

Laplace solutions in spherical coordinates were utilized for the derivation. Utilizing the displacement vector at the interfaces of the metal layer, dielectric core, and host matrix in addition to the continuity constraints of the potential, our aim, in this case, is to use these spherical coordinates as a basis to calculate the *EF* for spherical particles.

# 2.1. Dimensionless frequency and LFE factor in metal-covered spherical dielectric core analytically

It is assumed that the particle's dielectric function depends on both the local electric field and frequency. It can be stated as follows.

$$\varepsilon(\omega, E) = \varepsilon(\omega) + \chi |E|^2 \tag{6}$$

where  $\varepsilon(\omega, E)$  is a dielectric function as the function of frequency and electric field, and  $\chi$  is the Kerr coefficient. The optical behavior of a group of free electrons can be derived from the Lorentz harmonic oscillator model by effectively removing the springs, which is done by setting the spring constant k to zero. Therefore, for  $\omega$  is the incident frequency and dielectric function for free electrons is given by;

$$\varepsilon_m = \varepsilon_\infty - \frac{1}{z(z + i\gamma)} \tag{7}$$

Where  $\varepsilon_m$  is the dielectric function (*DF*) varies with the electron collision frequency,  $z = \omega / \omega_p$ 

is dimensionless frequency,  $\omega$  is the incident radiation frequency,  $\omega_p$  is the plasma frequency of the inclusion metal part,  $\nu$  is the electron collision frequency, and  $\gamma = \frac{\omega}{\omega_p}$ . The linear parts

of the DF is

$$\varepsilon_m = \varepsilon'_m + i\varepsilon''_m \tag{8}$$

Let's denote the parts, both real and imaginary of the equations above as follows:

$$\mathcal{E}'_{m} = \mathcal{E}'_{\infty} - \frac{1}{z^{2} + \gamma^{2}} \tag{9}$$

$$\varepsilon''_{m} = \varepsilon''_{\infty} + \frac{\gamma^{2}}{z(z^{2} + \gamma^{2})}$$
 (10)

By applying the continuity condition for both potential and displacement at the boundary interfaces, we determined the unknown variables A, B, C, and D as follows:

$$A = \frac{9\varepsilon_h \varepsilon_m}{2p\eta} \tag{11}$$

$$B = \frac{3\varepsilon_h(\varepsilon_d + 2\varepsilon_m)}{2\,pn}\tag{12}$$

$$C = \frac{3\varepsilon_h(\varepsilon_d - \varepsilon_m)}{2\,pn} r_1^3 \tag{13}$$

$$D = \left(1 - \frac{3p\varepsilon_h(\varepsilon_d - \varepsilon_m) + 9\varepsilon_h\varepsilon_m}{2p\eta}\right)r_2^3 \tag{14}$$

Hence, the enhancement factor (*EF*), which is complex, is formulated as follows:

$$A = \frac{9\varepsilon_h \varepsilon_m}{2p\eta} \tag{15}$$

where,

$$\eta = \varepsilon_m^2 + \prod \varepsilon_m + \varepsilon_d \varepsilon_h \tag{16}$$

$$\Pi = \left(\frac{3}{2p} - 1\right) \varepsilon_d + \left(\frac{3}{p} - 1\right) \varepsilon_h \tag{17}$$

$$p = 1 - \left(\frac{r_1}{r_2}\right)^3$$

Where p is a metal fraction in the inclusion,  $\epsilon_d$ ,  $\epsilon_m$ , and  $\epsilon_h$  are the dielectric functions of the core, metal, and host matrix, respectively.

Remember that the dielectric function of the core and metal-dielectric inclusions is provided by:

$$\varepsilon_m = \varepsilon'_m + i\varepsilon''_m \tag{18}$$

$$\varepsilon_{d} = \varepsilon'_{d} + i\varepsilon''_{d} \tag{19}$$

By squaring the EF and applying the modulus of Eq. (16), (17), and (18), we obtain

$$|A|^{2} = \frac{81\varepsilon_{h}^{2}}{4p^{2}} \frac{(\varepsilon'_{m}^{2} + \varepsilon''_{m}^{2})}{\eta'^{2} + \eta''^{2}}$$
(20)

Eq. (20) represents the *LFE* factor of the unknown coefficient in our original equation.

## 2.2. IOB in spherical metal-dielectric nanocomposite analytically

We now examine a spherical dielectric particle with radius  $r_1$ , enclosed by a metal enclosure of radius  $r_2$ . The core material is a nonlinear dielectric of the Kerr type, characterized by a nonlinear dielectric function.

$$\varepsilon_d = \varepsilon_d' + i\varepsilon_d'' + \chi |E|^2 \tag{21}$$

where  $\varepsilon_{d}'$  is the linear part of the dielectric function,  $\varepsilon_{d}''$  is the imaginary part (ImP) of the dielectric function of the core,  $\chi$  is the nonlinear Kerr coefficient, which generally varies with the frequency of the electromagnetic field, and E signifies the local field amplitude within the core. By substituting Eq. (17) and (21) into Eq. (16), we can reformulate it as:

$$\eta = \varepsilon_m^2 - \prod \varepsilon_m + (\varepsilon_{d0} + \chi |E|^2) \varepsilon_h$$

$$\eta = \varepsilon_m^2 - \varepsilon_m \prod_0 + \varepsilon_{d0} \varepsilon_h + \alpha \chi |E|^2$$

$$\eta = \eta_0 + \alpha \chi |E|^2 \tag{22}$$

Where

$$\eta_0 = \varepsilon_m^2 - \varepsilon_m \prod_0 + \varepsilon_{d0} \varepsilon_h$$

$$\eta_0 = \varepsilon_{d0} \left( \frac{3}{2p} - 1 \right) + \left( \frac{3}{p} - 1 \right) \varepsilon_h$$

$$\alpha = \varepsilon_m \left( \frac{3}{2p} - 1 \right) + \varepsilon_h$$

$$\eta_0 = \eta_0 + \eta_0 = \eta_0$$

$$\eta_0 = \eta_0' + i\eta_0''$$

$$\alpha = \alpha' + i\alpha''$$

$$\varepsilon_{d0} = \varepsilon_d' + i\varepsilon_d''$$

Substituting the above value for the EF into Eq. (20) and taking its modulus, we get

$$\left|A\right|^{2} = \frac{81}{4p^{2}} \frac{\left|\varepsilon_{m}\varepsilon_{h}\right|^{2}}{\alpha} \frac{1}{\left|\frac{\eta_{0}}{\alpha}\right|^{2} + 2\operatorname{Re}\left(\frac{\eta_{0}}{\alpha}\right)\chi\left|E\right|^{2} + \left|\chi\left|E\right|^{2}\right|^{2}}$$
(23)

The combination of all the above equations led us to locate the particle at the specific point, beginning with:

$$E = AE_h$$

Now by multiplying by  $\chi$  both sides of the above equation after squaring

$$\chi |E|^2 = |A|^2 \chi |E_h|^2 \tag{24}$$

By substituting the local field  $EF |A|^2$  into Eq. (24), we get

$$\chi \left| E_{lf} \right|^2 = \frac{81}{4p^2} \left| \frac{\varepsilon_m \varepsilon_h}{\alpha} \right|^2 \frac{\chi \left| E_h \right|^2}{\left| \frac{\eta_0}{\alpha} \right|^2 + 2 \operatorname{Re} \left( \frac{\eta_0}{\alpha} \right) \chi \left| E \right|^2 + \left| \chi \left| E \right|^2 \right|^2}$$
(25)

And letting  $\zeta = \chi |E|^2$ , and  $Y = \chi |E_h|^2$ , we acquire the following cubic equation for  $\zeta$ ;

$$\zeta = \frac{81}{4p^2} \left| \frac{\varepsilon_m \varepsilon_h}{\alpha} \right|^2 \frac{Y}{b + a\zeta + \zeta^2}$$

For the particle's local field computation, we derive the cubic equation;

$$\zeta^{3} + a\zeta^{2} + b\zeta = \phi Y$$
 (26) where,

$$a = 2\operatorname{Re}\left(\frac{\eta_0}{\alpha}\right), b = \left|\frac{\eta_0}{\alpha}\right|^2$$
$$\phi = \frac{81\varepsilon_h^2}{4p^2} \left|\frac{\varepsilon_m}{\alpha}\right|^2$$

Eq. (26) determines how the local field depends on the applied field; dimensionless frequency z, dielectric core, and other parameters of the system.

### 2.3. IOB domain in metal nanoparticles coated spherical dielectric core

The bistability domain in the plane  $(z, \chi |E_h|^2)$  can be specified from an examination of the roots of the cubic Eq. (26). Now, we analyze the roots of Eq. (26), and find the *IOB* domain in the plane  $(z, \chi |E_h|^2)$  and its solution is

$$Y = -\frac{2}{9\phi} \left( \Re\left(\frac{-a \pm \sqrt{\Re}}{3}\right) + \frac{ab}{2} \right)$$
 (27)

Let,  $Y=f(\alpha_i)$  and  $\Re = a-3b$  is the discriminant of  $Y'=f'(\alpha_i)=0$  And Eq. (27) becomes

$$f(\alpha_i) = -\frac{2}{9\phi} \left( \Re \alpha_i + \frac{ab}{2} \right)$$
 (28)

Where

$$\alpha_{1,2}\left(\frac{-a\mp\sqrt{\Re}}{3}\right), a\leq\sqrt{3b}, a<0.$$

One can write Eq. (28) as:

$$-\frac{2}{9\phi}\left(\Re a_2 + \frac{ab}{2}\right) < Y < -\frac{2}{9\phi}\left(\Re a_1 + \frac{ab}{2}\right) \tag{29}$$

 $\alpha_{1,2}$ , are the positions of extremum points of the function presented by the right component of Eq.

(28), they are determined from the equation  $3\alpha^2 + 2a\alpha + b = 0$ .

Below, we use the method developed, which allows one to study the shape and the bistability domain parameters in the  $(z, \chi |E_h|^2)$  plane. This domain is restricted by the curves.

$$f(\alpha_i) = -\frac{2}{9\phi} \left( \Re \alpha_i + \frac{ab}{2} \right)$$

Where.

$$a = 2 \operatorname{Re} \left( \frac{\eta_0}{\alpha} \right), b = \left| \frac{\eta_0}{\alpha} \right|^2, \quad \phi = \frac{81}{4 p^2} \left| \frac{\varepsilon_m \varepsilon_h}{\alpha} \right|^2$$

#### 3. Results and Discussion

### 3.1. LFE Factor in Metal Nanoparticles Covered Spherical Dielectric Core

The assumption is that the dielectric function of the particle varies with frequency and the local electric field E inside the particle, and it can be expressed in this form.

$$E = AE_h \tag{30}$$

Where A represents the enhancement factor determined as:

$$|A|^{2} = \frac{81\varepsilon_{h}^{2}}{4p^{2}} \left( \frac{\varepsilon_{m}^{2} + \varepsilon_{m}^{2}}{\eta^{2} + \eta^{2}} \right)$$
(31)

TD 11 1 T' C	1 ' 1			corresponding values
Table I tot of	nhucical	annontition along	with thoir	correction ding values
TADIC LASI OF	DHIVSICALI	UHAHIHES AIOHY	willi ilicii	COLLESDORIGHIS VALUES
I dole I. Dist of	pii, bicai	qualities arong	TTTT CITCII	corresponding varaes

Used Parameters		Value assigned		
$\mathcal{E}_h$		2.25		
$\mathcal{E}_d$ '		6.0		
$\mathcal{E}_{\infty}$ '		4.6		
$\omega_h$		$1.4\times10^{16}$		
v		$1.68 \times 10^{14}$		
γ		$1.15x10^{-2}$		
$\mathcal{E}_{_{\infty}}$ "		0		
p		0.4 - 0.95		
z		0.10 - 0.50		

The numerical values listed in Table 1 were utilized to plot the enhancement factor (*EF*) by varying the *ImP* of the dielectric function of the core against the dimensionless frequency z in the figure below.

The LFE factor varies with dimensionless frequency, as depicted in the following figures;  $|A|^2$  versus z. Figure 2 illustrates that  $|A|^2$  exhibits two peak values at distinct resonant frequencies for a nanocomposite containing metal-coated dielectric spherical nano-inclusions. The presence two resonant frequencies corresponds to interactions between the metallic part of the inclusion and the two dielectric components of the composite. The metal shell interfaces with both the host dielectric and the dielectric core. Consequently, the free electrons of the metal fluctuate at various surface Plasmon frequencies at the interfaces between the dielectric host matrix and the dielectric core. This results in a significant increase in the LFE factor at these two resonant frequencies.

Figure 2 explains that the center of the spherical nanoparticle has to preserve the tuned DF  $\varepsilon_d$  of the core. By fixing the imaginary part (ImP) of the dielectric function of the core  $\varepsilon_d$ " as an example at point  $\varepsilon_d$ " = 0.0, -0.10, -0.2, -0.25, and -0.3 the ImP  $\varepsilon_d$ " of the dielectric core plays a

basic role for enhancement factor (*EF*) of the local field. As a result, the electric field enhancement of the local field increased for the metallic dielectric function when an additional dielectric function was applied to the imaginary part of the active dielectric properties of the core, as depicted in Figure 2.

Figures 3 and 4 depict the *EF* of composites consisting of small spherical metal-dielectric structures separated by a metal layer, plotted against the metal fraction *p* for various distinct values of the dielectric core. Both the dimensionless metal fraction *p* and the dielectric core play pivotal roles in enhancing the local field through resonant frequency tuning. Figure 4 demonstrates that composites containing dielectric spherical nano-inclusions coated with metal exhibit a singular resonant frequency and a maximum enhancement factor value.

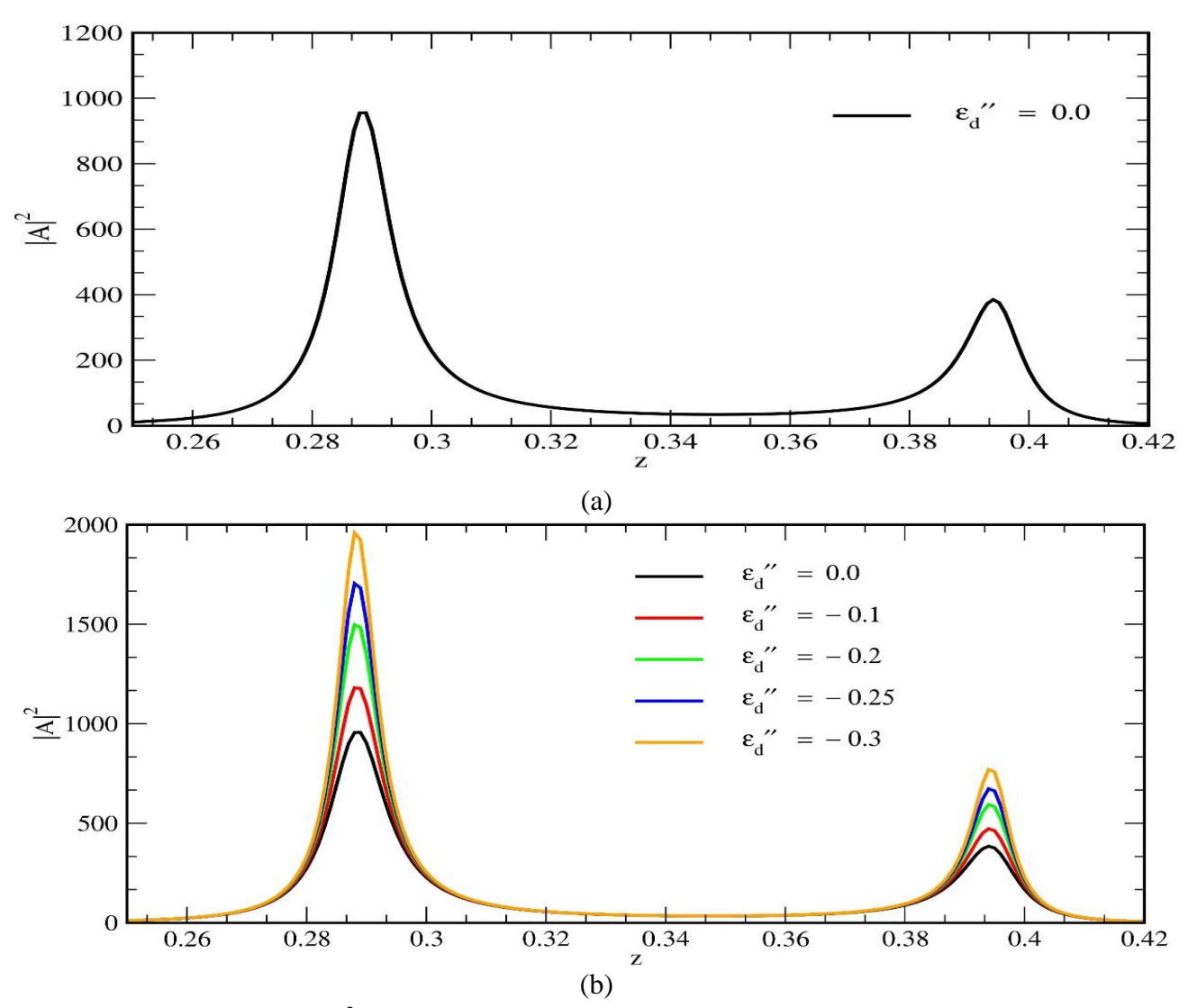


Figure 2: The LFE factor  $|A|^2$  for spherical nanoparticle versus z in linear host matrix: a) at p=0.9 and for  $\varepsilon_d'' = 0.0$ ; b) for different values of  $\varepsilon_d''$ , where the rest quantities are the same as Table 1

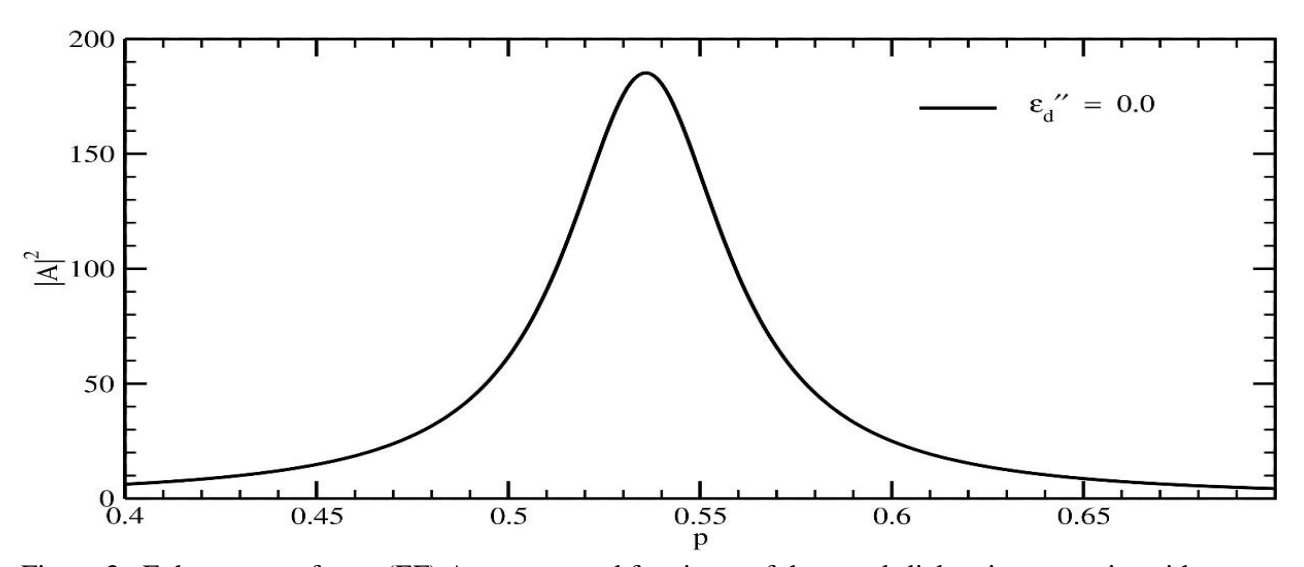


Figure 3: Enhancement factor (EF) A versus metal fraction p of the metal-dielectric composite with  $\varepsilon_d'' = 0.0$ .

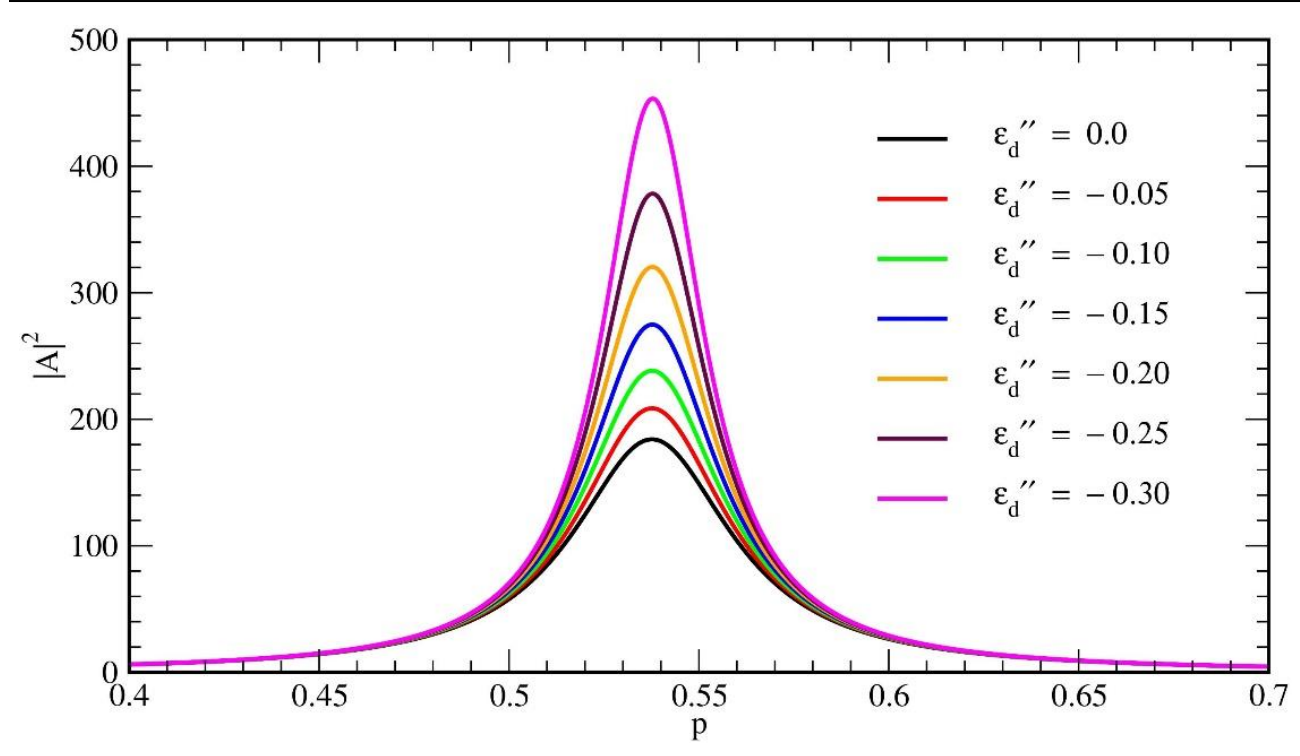


Figure 4: LFE factor  $|A|^2$  versus metal fraction p of the metal-dielectric composite with different dielectric  $\varepsilon_d$ " at z=0.2.

The imaginary component of the core can be altered in this kind of composite to enhance the electric field. Figure 4 clearly shows that the *LFE* factor increases as the additional dielectric function added to the dielectric properties of the core increases.

### 3.2. IOB in spherical metal-dielectric nanoparticles

The *EF* relies on the local field *E*, therefore, incorporating the nonlinear term from Eq. (32) is essential for the significant *LFE* within the coated spherical nanoparticles. The computation of the local field  $(\chi |E|^2)$  in the particle follows the method described in the second section, employing the cubic equation.

$$\zeta^3 + a\zeta^2 + b\zeta = \phi Y \tag{32}$$

where, 
$$a = 2 \operatorname{Re} \left( \frac{\eta_0}{\alpha} \right), b = \left| \frac{\eta_0}{\alpha} \right|^2$$
 and

$$\phi = \frac{81}{4p^2} \left| \frac{\varepsilon_m \varepsilon_h}{\alpha} \right|^2$$

Eq. (32) establishes the link between the local field, the applied field Y, dimensionless frequency z, the dielectric core, and other system parameters. By utilizing Eq. (32), we constructed the optical bistability curve. The adjustment of dielectric properties in the core enhances the understanding of optical bistability in spherical composites by providing more precise control over the electromagnetic response of the material. Optical bistability, where the material can exist in two distinct optical states, is highly delicate to the dielectric environment. By finely tuning the core's dielectric properties, we can observe and manipulate the interaction between the nanocomposite and the light material more accurately.

From Figure 5, we understand that when we supply intensity from an external source, we get two stable output intensities. Therefore, from Eq. (32) this stability we called bistability which is a real number, and there is one imaginary part (ImP) that is absorbed. The passive dielectric function (DF) core, the natural property of the

*DF* of the dielectric of the core is not affected by applying additional dielectric function, then  $\varepsilon_d'' = 0$ . The graph of Eq. (32) depicting a

spherical metal-dielectric nanocomposite within a passive *DF* of the core is illustrated in Figure 5.

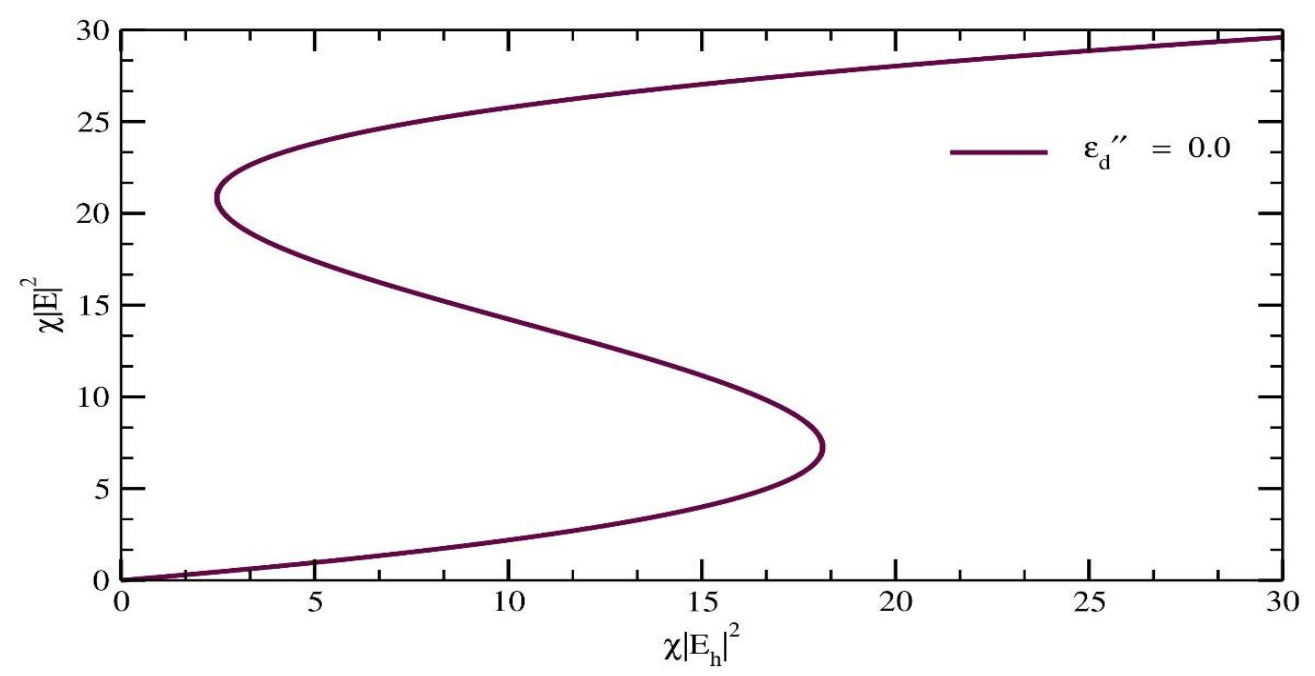


Figure 5: IOB of spherical metal-dielectric nanocomposites in a linear host matrix at p=0.9 and z=0.2.

This configuration is indicated by the term *IOB*, typically represented in the *Y-X* plane. It is characterized by *S*-shaped curves, indicating that

three distinct local field values equate to one applied field value.

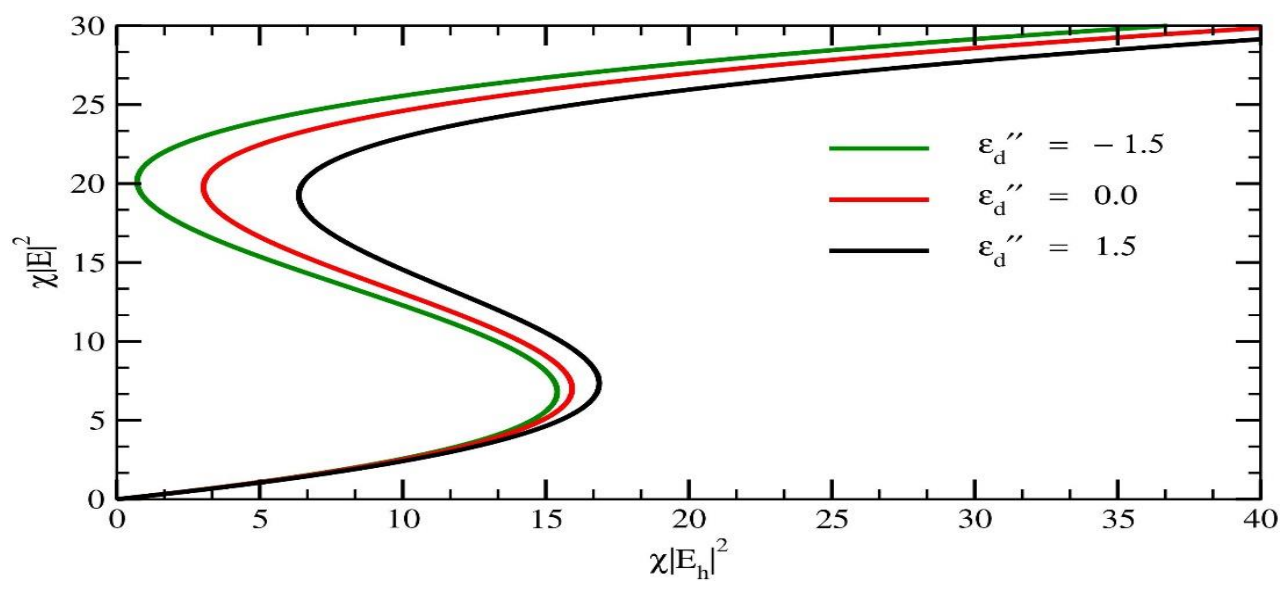


Figure 6: (Color online) IOB of spherical metal-dielectric nanocomposites in a linear host matrix at p=0.9, z = 0.2 and for different  $\mathcal{E}_d$  with the rest parameters as in Table 1.

The graph depicted in Figure 6 was generated using Eq. (32) and illustrates the parameter region where three distinct values of the local field correspond to a single value of the applied

field. Optical bistability frequently depends on nonlinear optical effects occurring within the material. Modifying the dielectric properties in the core can enhance these nonlinear responses, making the bistability more pronounced or modifying the form of the bistable curve (hysteresis loop). This enhancement provides insights into the underlying mechanisms governing the optical switching dynamics.

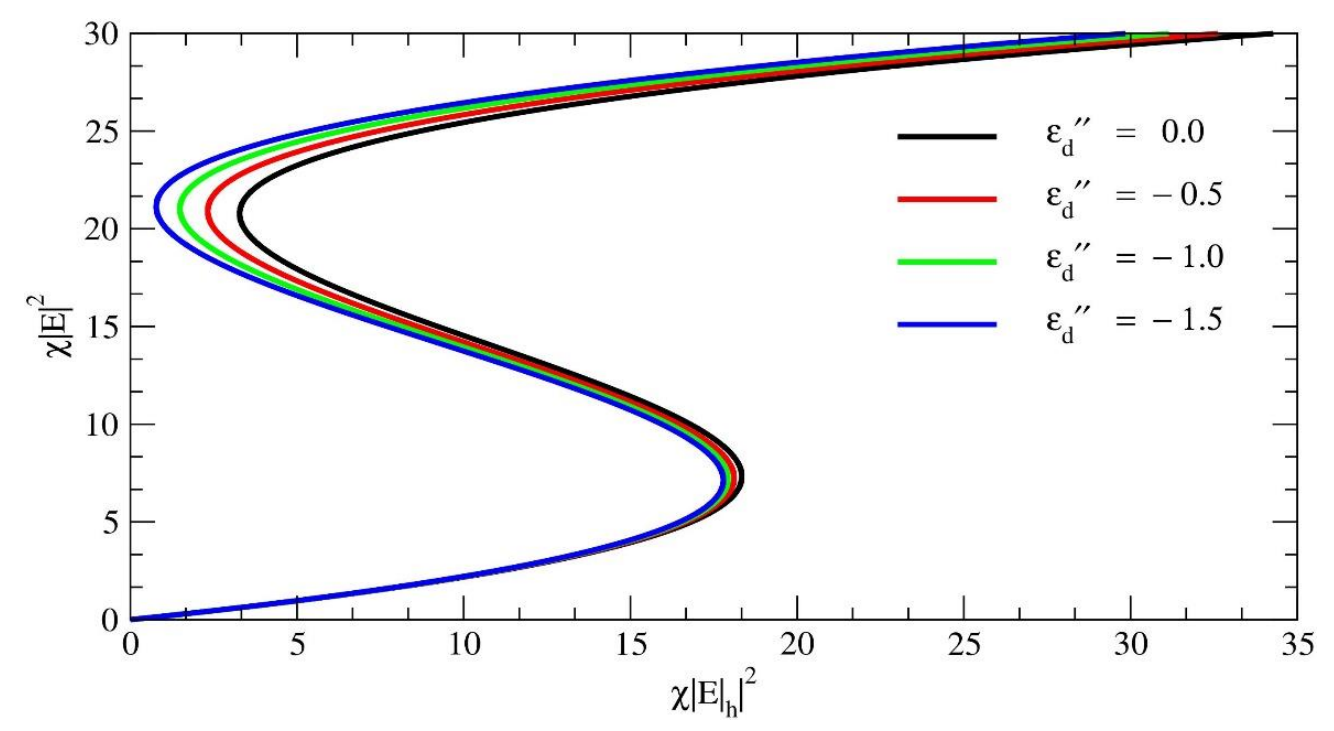


Figure 7: (Color online) IOB of spherical metal-dielectric nanocomposites in a linear host matrix for four different  $\mathcal{E}_d$ " at z = 0.2 and p=0.9.

From Figures 6 and 7, we have seen that in the active dielectric core, the ImP of the dielectric function of the dielectric core  $(\varepsilon_d'')$  is affected by applying an additional dielectric function (DF) on it, which is like that of increasing the density of the small spherical metal-dielectric composite particle, then  $\varepsilon_d'' \neq 0$ . By comparing three different values of the local field to one value of the applied field, it is possible to see that the bistability region expands as an ImP of the DF of the core dielectric applying an additional DF on it. The negative sign indicates the introduction of an additional DF to the core dielectric. Figures 6 and 7 illustrate that as the ImP of the dielectric function of the dielectric core increases due to this additional function, the range of optical bistability (threshold width) expands, enhancing system oscillation (increasing system activation). The dielectric properties significantly affect the of resonance conditions the composite nanoparticles. By adjusting the core's dielectric

constant, one can shift the plasmon resonance frequency. This shift affects the interaction between the incident light and the composite, altering the conditions under which optical bistability occurs.

Based on Figure 7, we noticed that by modifying the imaginary component of the *DF* of the active dielectric properties core through the application of an additional dielectric function, it is akin to increasing the density of small spherical metal-dielectric structures. Consequently, varying amplitudes of maximum values are achieved at the same dimensionless resonance frequency.

The graph shown in Figure 8 is generated using Eq. (32), illustrating an intriguing range of parameters where three distinct values of the local field  $(\chi |E|^2)$  align with a single value of the applied field  $(\chi |E_h|^2)$ . When analyzing bistability phenomena within the system, it is advantageous

to examine how the local field varies with the applied field. These relationships, derived from Eq. (32) at z=0.2 for three different metal fractions within the inclusion, demonstrate that the region of bistability (where three different

values correspond to one value) significantly widens as the proportion of the metal shell coating the active dielectric core in the inclusion increases.

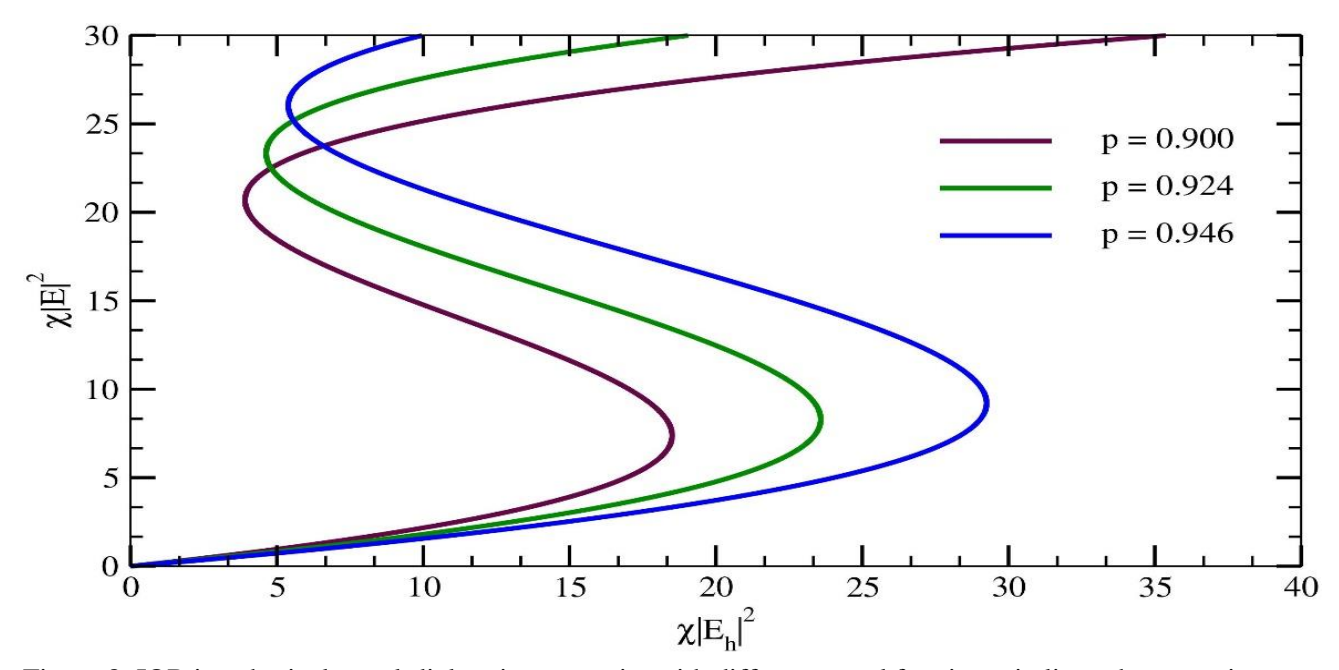


Figure 8: IOB in spherical metal-dielectric composite with different metal fraction p in linear host matrix at z = 0.2, p = 0.9, and  $\varepsilon_d'' = -0.3$ 

It is important to emphasize that the present study is the first to examine the impact of tuning the dielectric core on the LFE factor, optically induced bistability and its domain in spherical nanocomposites. Most existing studies have focused on parameters such as metal fraction, depolarization, and interfacial layers in spherical metal-dielectric nanocomposites, without considering the adjustment of the ImP of the dielectric core. In comparison with recent studies by (Bergaga et al, 2022; Getachew, 2024; Shewamare and Mal'nev, 2012) on metaldielectric spherical nanocomposites, our study demonstrates that the LFE factor increases at specific resonant frequencies under the same metal fraction and dielectric constant. However, it is important to note that these previous studies did not account for the real and imaginary parts of the linear DF of the core. Our findings suggest that by tuning the active dielectric properties of the core, we can enhance the local field and

increase the threshold width of optical bistability in metal-dielectric spherical nanocomposites, thereby improving the activation of the system.

### 3.3. IOB domain in spherical metal-dielectric composite nanoparticles

The curve  $f(\alpha_1)$  presents a set of maxima of  $\phi Y$  and the curve  $f(\alpha_2)$  presents a set minima of  $\phi Y$  in the z,  $\chi |E_h|^2$  plane. We note that the curves  $\phi Y$  are unlike the *S*-type curves $\alpha$ . If positions of maxima and minima coincide, the curves  $f(\alpha_{1,2})$  merge, and there is no bistability at all.

Figures 9b and 10b show the IOB regions of the solution to cubic Eq. (32), illustrating typical dependencies of the local field on the applied field. We applied several additional ImPs of the DF to the active dielectric core, ranging from 0.0 to -1.0, at a specific resonant frequency z=0.2, to illustrate the IOB domains. Below, we present

typical dependencies of the local field on the applied field (Figures 9a and 10a), obtained from cubic Eq. (32), and *IOB* domains (Figures 11b and 12b) derived from bistability conditions Eq. (29). We obtained IOB domains for two different additional dielectric functions applied to ImP of the dielectric core  $\varepsilon_d$ " at  $\varepsilon_d$ ' = 6.0. From Figures 9 and 10, it is evident that the onset and offset of optical bistability described by Eq. (32) correspond to the bistability domain condition

illustrated in Eq. (29). The amplitude between the onset and offset of IOB shown in these figures is equivalent to the distance between the minima and maxima  $\Phi Y$  which is calculated from the solution of the cubic equation at a specific resonance frequency z=0.2. According to the findings, the bistability domain expands with an increase in the additional dielectric function in the ImP of the active DF of the core.

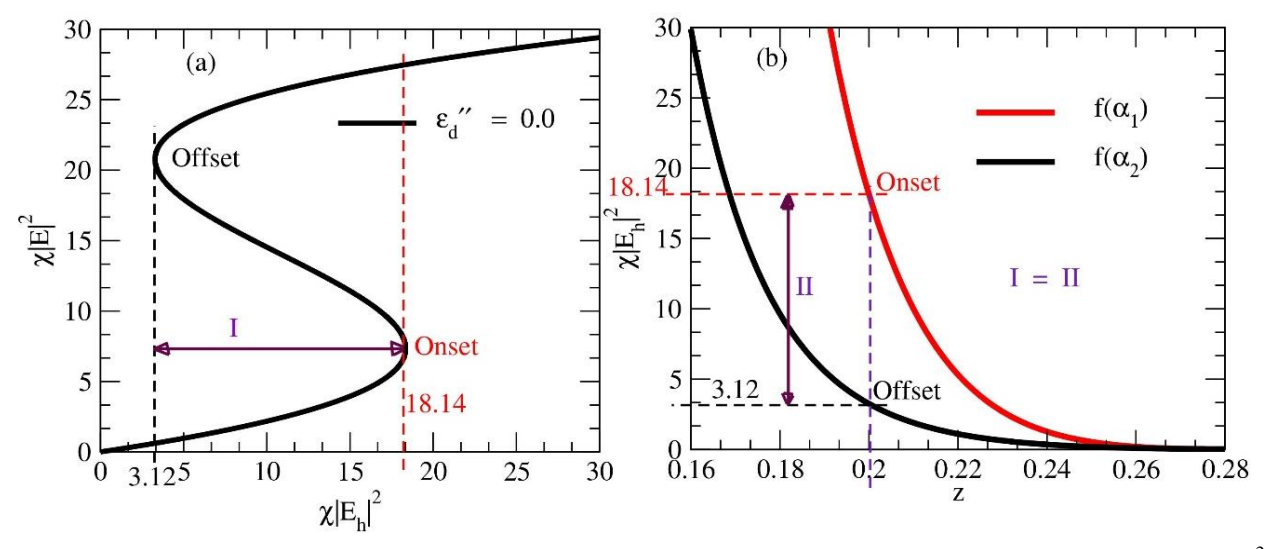


Figure 9: IOB in the coated spherical particle: at z=0.2,  $\varepsilon_d''=0.0$  and p=0.9; a) The applied field  $(\chi|E_h|^2)$  versus the local field  $(\chi|E|^2)$ ; b) IOB domain in the plane  $(z, \chi|E_h|^2)$ 

The curves  $f(\alpha_1)$  and  $f(\alpha_2)$  are calculated with the help of Eq. (32).

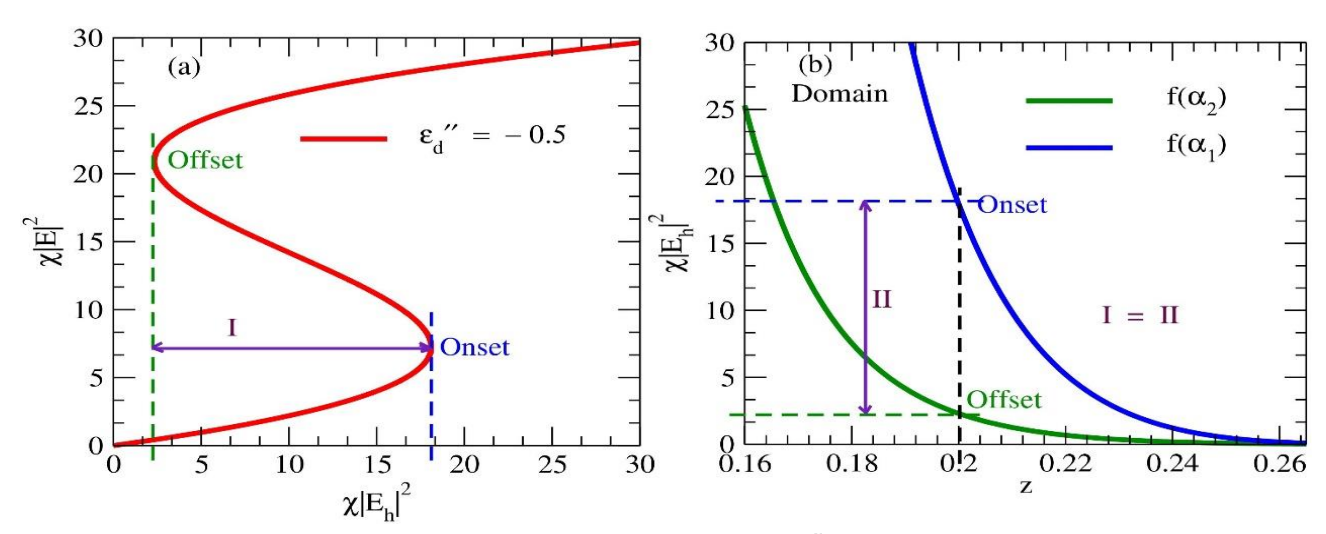


Figure 10: IOB in the coated spherical nanocomposite at z=0.2,  $\varepsilon_d''=-0.5$  and p=0.9; a) The applied field  $(\chi |E_h|^2)$  versus the local field  $(\chi |E|^2)$ ; b) IOB domain in the plane  $(z, \chi |E_h|^2)$ 

These results have practical implications for the design of advanced photonic devices such as optical switches, modulators, and sensors. The ability to control and expand the bistability region through the manipulation of the dielectric

function of the core means that devices can be engineered to operate more reliably at specific resonant frequencies. This can lead to improved performance in terms of switching speed, sensitivity, and energy efficiency.

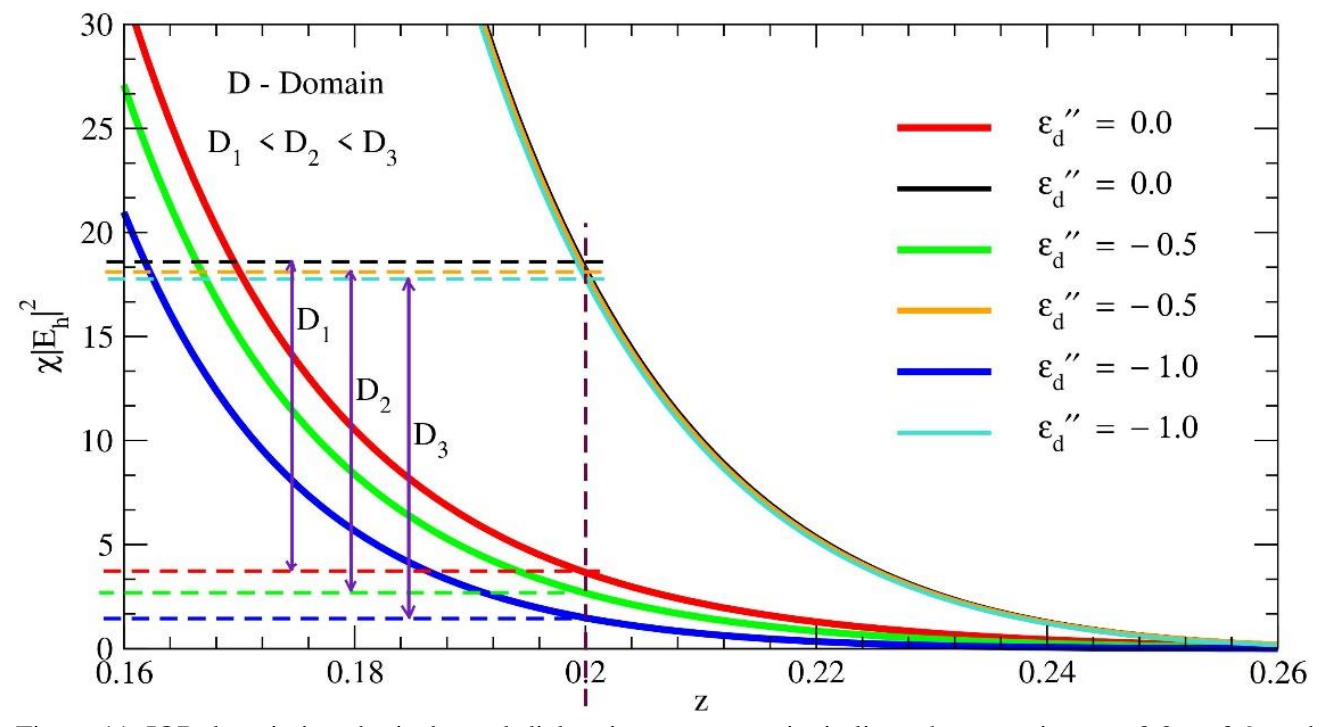


Figure 11: IOB domain in spherical metal-dielectric nanocomposite in linear host matrix at z= 0.2, p=0.9, and for different  $\epsilon_d$ "

Figure 11 illustrates the dependencies of the IOB domain on the ImP of the active dielectric core, determined by solving the cubic equation (32). The curves enclosing the bistability domain provide information similar to S-type curves, indicating onset and offset bistability fields at specific frequencies. These results show that as the ImP of the dielectric function of the core (denoted as  $\varepsilon_d$ ") varies (at values 0.0, -0.5, and -1.0), the domain of IOB expands. This suggests that modifying the additional dielectric function on the ImP of the dielectric core alters the optical properties of the system, potentially shifting its energy from red to blue wavelengths.

### 4. Summary and Conclusion

This study investigates the impact of tunable dielectric properties of the core on enhancement factor (*EF*) local field and induced optically

induced bistability and its domain in spherical metal-dielectric nanocomposites. The dielectric function of the metal-coated dielectric core significantly influences the enhancement factor, exhibiting two distinct peaks at dimensionless frequencies. The *EF* of the local field increases notably at these resonant frequencies as the magnitude of the active dielectric core increases negatively. The negative sign of the *ImP* of the active dielectric properties of the core implies an additional dielectric function (*DF*) applied to the core, thereby enhancing the local field factor for metallic *DF*. Hence, the behavior of enhancing the local field is profoundly influenced by the *ImP* of the dielectric core.

Furthermore, the adjustable dielectric properties of the core impact the optical bistability observed by modifying local field enhancement, shifting resonant frequencies, and nonlinear interactions. Introducing an extra dielectric function to the imaginary part of the active dielectric core decreases absorption, enhances local field strength, and reinforces the material's nonlinear optical reaction. This outcome widens the bistability region, enabling the system to display bistable characteristics across a broader range of applied fields.

The results suggest that the OB domain expands as the ImP of the dielectric function of the dielectric core increases through the application of an additional dielectric function. This enhancement facilitates increased activation of the system. These discoveries suggest potential

applications for speeding up optical computing and communication technologies while improving their energy efficiency. Additionally, they have the potential to lead to significant advancements in quantum information processing, optical switches, and sensing capabilities.

### **Data Availability Statement**

This manuscript has no associated data or the data will not be deposited.

### **Conflicts of Interest**

The authors have no conflicts to declare.

#### References

- Amendola, V., Pilot, R., Frasconi, M., Maragò, M., & Iatì, A. (2017). Surface plasmon resonance in gold nanoparticles: A review. Journal of Physics. Condensed Matter. 29(20):203002. http://dx.doi.org/10.1088/1361-648X/aa60f3
- Anker, J., Hall, P., Lyandres, O., & Shah, C. (2008). Biosensing with plasmonic nanosensors. Nature Materials 7(6):442-453. http://dx.doi.org/10.1038/nmat2162
- Arnold, T., O'Keeffe, R., Leung, K., Folan, L., Scalese, T., & Pluchino, A. (1990). Optical bistability of an aqueous aerosol particle detected through light scattering: Theory and experiment. Applied Optics. 29 (24), 3473-3478. https://doi.org/10.1364/ao.29.003473
- Bennink, R. S., Yoon, Y. K., Boyd, R. W., & Sipe, J. E. (1999). Accessing the optical nonlinearity of metals with metal-dielectric photonic bandgap structures. Optics Letters, 24(20), 1416-1418. https://doi.org/10.1364/OL.24.001416
- Bergaga, G. D., Ali, B. M., & Debela, T. S. (2022). Size-dependent local field enhancement factor of CdSe based core@ shell spherical nanoparticles. Materials Research Express, 9(4), 045001. http://dx.doi.org/10.1088/2053-1591/ac60e2
- Chen, H. L., Gao, D. L., & Gao, L. (2016). Effective nonlinear optical properties and optical bistability in composite media containing spherical particles with different sizes. Optics express, 24(5), 5334-5345. https://doi.org/10.1364/OE.24.005334
- Daneshfar, N., & Bazyari, K. (2014). Optical and spectral tunability of multilayer spherical and cylindrical nanoshells. Applied Physics A, 116, 611-620. https://doi.org/10.1007/s00339-013-8188-z
- Daneshfar, N., & Naseri, T. (2017). Switching between optical bistability and multistability in plasmonic multilayer nanoparticles. Journal of Applied Physics, 121(2). https://doi.org/10.1063/1.4973961
- Gao, L. (2003). Optical bistability in composite media with nonlinear coated inclusions. Physics Letters A, 318(1-2), 119-125. https://doi.org/10.1016/j.physleta.2003.09.025
- Getachew, S. (2024). Effect of Tunable Dielectric Core on Optical Bistability in Cylindrical Core-Shell Nanocomposites. Advances in Condensed Matter Physics, 2024(1), 9911970. https://doi.org/10.1155/2024/9911970

- Getachew, S., & Berga, G. (2024). Investigating the optical bistability of pure spheroidal nanoinclusions in passive and active host matrices. Canadian Journal of Physics. https://doi.org/10.1139/cjp-2024-0144
- Getachew, S., Shewamare, S., Diriba, T., & Birhanu, G. (2023). Local field enhancement of cylindrical core—shell nanoparticle composites in passive and active dielectric core. International Journal of Current Research, 15(11), 26432-26438. https://doi.org/10.24941/ijcr.45824.11.2023
- Kalyaniwalla, N., Haus, J. W., Inguva, R., & Birnboim, M. H. (1990). Intrinsic optical bistability for coated spheroidal particles. Physical Review A, 42(9), 5613. https://doi.org/10.1103/PhysRevA.42.5613
- Lisiecki, I., Billoudet, F., & Pileni, M. P. (1996). Control of the shape and the size of copper metallic particles. The Journal of Physical Chemistry, 100(10), 4160-4166. https://doi.org/10.1021/jp9523837
- Lv, W., Phelan, P. E., Swaminathan, R., Otanicar, T. P., & Taylor, R. A. (2013). Multifunctional coreshell nanoparticle suspensions for efficient absorption. Journal of solar energy engineering, 135(2), 021004. https://doi.org/10.1115/1.4007845
- Mahmudin, L., Suharyadi, E., Utomo, A. B. S., & Abraha, K. (2015). Optical properties of silver nanoparticles for surface plasmon resonance (SPR)-based biosensor applications. Journal of Modern Physics, 6(08), 1071.
- Nugroho, B. S., Iskandar, A. A., Malyshev, V. A., & Knoester, J. (2020). Plasmon-assisted two-photon absorption in a semiconductor quantum dot—metallic nanoshell composite. Physical Review B, 102(4), 045405. https://doi.org/10.1103/PhysRevB.102.045405
- Piralaee, M., Asgari, A., & Siahpoush, V. (2018). Plasmonic properties of spheroid silicon-silver nanoshells in prolate and oblate forms. Optik, 172, 1064-1068. https://doi.org/10.1016/j.ijleo.2018.07.131
- Shewamare, S., & Mal'nev, V. N. (2012). Two optical bistability domains in composites of metal nanoparticles with nonlinear dielectric core. Physica B: Condensed Matter, 407(24), 4837-4842. https://doi.org/10.1016/j.physb.2012.08.007
- Stalmashonak, A., Seifert, G., & Abdolvand, A. (2013). Ultra-short pulsed laser engineered metal-glass nanocomposites (pp. 5-15). New York, NY, USA: Springer. http://dx.doi.org/10.1007/978-3-319-00437-2
- Van Thourhout, D., & Roels, J. (2010). Optomechanical device actuation through the optical gradient force. Nature Photonics, 4(4), 211-217. http://dx.doi.org/10.1038/nphoton.2010.72
- Volz, T., Reinhard, A., Winger, M., Badolato, A., Hennessy, K. J., Hu, E. L., & Imamoğlu, A. (2012). Ultrafast all-optical switching by single photons. Nature Photonics, 6(9), 605-609. https://doi.org/10.1038/nphoton.2012.181
- Zhang, Y. X., & Wang, Y. H. (2017). Nonlinear optical properties of metal nanoparticles: a review. RSC advances, 7(71), 45129-45144. https://doi.org/10.1039/C7RA07551K
- Zhu, J., & Zhao, S. M. (2016). Plasmonic refractive index sensitivity of ellipsoidal Al nanoshell: Tuning the wavelength position and width of spectral dip. Sensors and Actuators B: Chemical, 232, 469-476. https://doi.org/10.1016/j.snb.2016.03.163